

Postprint: Microstructure Evolution Mechanism and Mechanical Properties of FeNiCrAl Alloy Strengthened by Coherent NiAl via Aluminothermic Synthesis

Authors: Wang Xing, Xi Wenjun, Cui Yue, Li Shujie

Date: 2016-11-04T00:00:00+00:00

Abstract

The microstructure of FeNiCrAl alloy prepared by aluminothermic synthesis was investigated using XRD, SEM, TEM, and other experimental methods, and the effect of Al content in the thermite composition on the tensile properties of the alloy was studied. The results show that when the Al content in the thermite does not exceed 25.4%, the main constituent phase of the alloy is austenite; when the Al content in the thermite reaches 26.6%, the main constituent phase changes to ferrite, accompanied by the precipitation of a granular NiAl phase; as the Al content continues to increase, the granular precipitate phase is gradually replaced by a woven-like structure. Analysis indicates that the formation of the woven-like structure results from spinodal decomposition in the liquid phase. Increasing the Al content in the thermite decreases the elongation after fracture of the alloy. When the Al content in the thermite is 26.6%, the tensile strength of the alloy reaches its maximum value of 640.87 MPa.

Full Text

Preamble

ACTA METALLURGICA SINICA

Microstructure Evolution Mechanism and Mechanical Properties of FeNiCrAl Alloy Reinforced by Coherent NiAl Synthesized by Thermite Process

WANG Xing, XI Wenjun*, CUI Yue, LI Shujie

(School of Materials Science and Engineering, Beihang University, Beijing 100191)

ABSTRACT

The excellent thermal conductivity, low thermal expansion, and high oxidation resistance of ferritic FeNiCrAl alloys provide them with the potential to replace nickel-based superalloys in high-temperature applications. However, their usage is limited by poor high-temperature mechanical properties. The high melting point of NiAl intermetallic compounds, together with their excellent high-temperature stability and similar lattice parameters to γ -Fe, allows them to coherently strengthen ferritic FeNiCrAl alloys and extend their high-temperature performance. Traditionally, these Fe(Ni,Cr)/NiAl alloys are prepared by vacuum reaction melting followed by an aging process. However, the aging process has drawbacks including excessive cost, lengthy aging times, and coarsening of the NiAl phase at high temperature.

A more cost-effective thermite reaction process was attempted to prepare the Fe(Ni,Cr)/NiAl alloys. In this route, ferritic FeNiCrAl alloys were strengthened by a high volume fraction of nanoscale NiAl phase achieved without using the aging process. Several types of thermites were designed, and studies were conducted to explore the transformations of alloy microstructures and changes in tensile properties with various thermite compositions.

The microstructures of these thermite-synthesized Fe(Ni,Cr)/NiAl alloys were investigated using XRD, SEM, EDS, TEM, and SAED. The effect of Al content in the thermites on alloy microstructures was studied. Experimental results showed that when the thermites contained no more than 25.4 mass% Al, the synthesized Fe(Ni,Cr)/NiAl alloys were composed primarily of an austenite phase. The main component phase of the alloy composites transformed into ferrite when the mass fraction of Al in the thermites reached 26.6%, while NiAl particle precipitates arose simultaneously. As the Al content of the mixture was further increased, the NiAl precipitates were gradually replaced by an intertexture structure. The intertexture structure became totally dominant when the mass fraction of Al in the thermites reached 31.4%. Experimental results showed that this intertexture microstructure material was composed of a ferritic FeNiCrAl matrix with a width of 80–100 nm and NiAl precipitates with a width of about 50 nm, and the two phases matched coherently. This microstructure resulted from liquid spinodal decomposition.

The effect of Al content on the mechanical properties of the alloys was also investigated. The increase of Al content in the thermites resulted in a decrease in alloy elongation, which varied from 25.5% to 1.7% when the mass fraction of Al ranged from 24.2% to 29.0%. When the thermites contained 26.6 mass% Al, the tensile strength of the alloy achieved its maximum value of 640.87 MPa.

KEY WORDS Thermite process; NiAl; Tensile properties; Liquid spinodal decomposition

Ferritic heat-resistant steels offer promising applications in the nuclear industry and future fusion reactors due to their lower thermal expansion coefficient, superior high-temperature oxidation resistance, higher thermal conductivity, better

radiation damage performance, and lower cost compared to austenitic heat-resistant steels. However, their high-temperature strength and creep resistance above 600°C are relatively poor, limiting their application scope [1]. Research [2] has shown that the high-temperature creep resistance of ferritic alloys can be effectively improved through two-phase coherent strengthening mechanisms. The B2-structured NiAl intermetallic compound has a bcc structure like α -Fe, and its lattice constant (0.28864 nm) is extremely close to that of α -Fe (0.28665 nm) [3], thus satisfying the requirements for serving as a coherent strengthening phase in bcc-structured iron-based alloys and achieving a α -' coherent strengthening microstructure similar to that in nickel-based superalloys [4,5].

Currently, the preparation of coherently precipitated Fe-Ni-Al alloy systems is mainly achieved through vacuum reaction melting and aging. Calderon et al. [2,6] conducted extensive studies on the aging behavior of Fe-Ni-Al alloys at different temperatures and times, and discussed the coarsening kinetics of the system. To improve the oxidation resistance of the alloy system, Hao et al. [7] added Cr to the Fe-Ni-Al system and found that Cr would almost completely dissolve in α -Fe. Fe-Ni-Cr-Al alloys combine the excellent oxidation resistance of ferritic Fe-Cr-Al alloys with the superior high-temperature strength of Fe-Ni-Al alloys containing high volume fractions of the B2 phase. By precipitating NiAl ordered phases in the iron matrix, they have the potential to serve as a new type of high-performance high-temperature structural material [8]. Vo et al. [9] thoroughly investigated the microstructure of aged Fe-Ni-Cr-Al alloys, statistically analyzed the volume fraction and size of NiAl precipitates in α -Fe, and studied their microstructural and property changes after high-temperature creep.

Bradley et al. [10], through phase diagram and thermodynamic studies of the system, concluded that with sufficient Al provision, the volume fraction of NiAl precipitates in α -Fe could vary over a wide range. Stallybrass et al. [8] aged Fe-Ni-Cr-Al alloy samples at 900°C for 100 h and found that as the Al and Ni content in the raw materials increased, the NiAl precipitates not only increased in volume fraction but also gradually changed from a particle shape to a previously unobserved intertexture structure. They studied the compressive yield strength of this alloy at high temperature but did not explain the formation mechanism of this intertexture structure.

The method of preparing NiAl-coherently strengthened Fe-Ni-Cr-Al alloys through aging still suffers from problems such as excessively long cycles, high production costs, and coarsening of the NiAl phase during prolonged high-temperature aging. Therefore, researchers continue to explore new preparation methods for Fe-Ni-Cr-Al alloys. Combustion synthesis technology, as a method for preparing high-temperature, refractory, and wear-resistant materials, has attracted increasing attention from scholars worldwide due to its low cost, energy efficiency, and simple equipment, particularly when combined with traditional processes such as centrifugal casting [11-14]. In this work, Fe-Ni-Cr-Al alloys were prepared through thermite reaction combustion

synthesis. This process is simple, has short reaction times, and can produce ferritic alloys strengthened by nanoscale, high-volume-fraction NiAl phases without using an aging process, avoiding the long duration, high cost, and NiAl phase coarsening associated with prolonged aging. By increasing the Al content in the thermite, the intertexture microstructure observed by Stallybrass et al. [8] through aging methods also appeared in the samples. This work attempts to discuss the formation mechanism of this intertexture structure and investigate the influence of varying Al content in the thermite on sample microstructure and tensile properties.

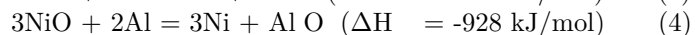
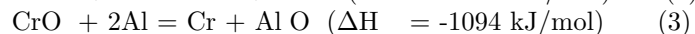
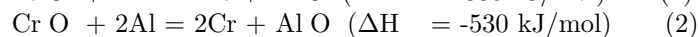
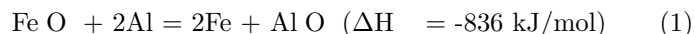
1 Experimental Methods

Fe(Ni,Cr)/NiAl alloys were synthesized using a thermite reaction process with Fe O , NiO, Cr O , CrO , and Al as thermite raw materials. To ensure that the obtained alloys could satisfy the thermodynamic conditions for coexistence of -Fe and NiAl phases and to generate sufficient heat for a more complete reaction, the thermite compositions used in this experiment were designed based on relevant phase diagrams [15] and Thermo-Calc thermodynamic software, as shown in . The Al content (as a reducing agent) varied across compositions while other components remained constant. The total mass of thermite used in each experiment was 500 g.

The main sample preparation procedure was as follows: The thermite powders were ground and mixed uniformly, placed in a graphite crucible (with a small hole at the bottom) sealed with Al foil, and wrapped with insulation material to prevent heat loss. The crucible with insulation was placed in a drying oven and held at 120°C for 2 h before removal.

The thermite reaction synthesis apparatus is shown in [Figure 1: see original paper]. The graphite crucible was placed on a Cu mold with a ceramic filter inserted in between to filter out impurities generated during the reaction. The powder mixture was ignited with a heated W wire. Once ignited, the redox reaction proceeded and was sustained by the heat released from the reaction.

The chemical reactions during the process are complex, but the main reactions are generally considered to be:



where ΔH represents the heat released per mole of reaction at room temperature. Equations (1)-(4) show that the main reaction products are Fe, Ni, Cr, and Al O . The reaction releases substantial heat, melting all products. Al O has low density and poor wettability with the FeNiCrAl alloy melt, giving it a tendency to separate from the melt under gravity. Due to the extremely high temperatures achieved during the thermite reaction, Al O has sufficient time to

float out of the alloy during melt solidification, forming an Al₂O₃ slag layer. After solidification, macroscopic separation between Al₂O₃ and the alloy is complete, and the alloy sample is obtained by removing the upper Al₂O₃ slag layer.

During the reaction, the high-temperature melt melted through the Al foil, poured into the pre-placed Cu mold, and after solidification, the surface Al₂O₃ slag layer was removed to obtain the alloy sample. The resulting alloy samples were cylindrical with a diameter of approximately 16 mm, length of about 120 mm, and mass of about 150 g. The mass loss originated from separation of impurities and material splashing/residue in the mold during the reaction.

The alloy microstructure was observed using a JSM-6010LA scanning electron microscope (SEM) and an Apollo-300 field-emission SEM. A JEM-2100F transmission electron microscope (TEM) combined with selected-area electron diffraction (SAED) and energy-dispersive spectroscopy (EDS) was used for further investigation of microstructural morphology and phase composition. Microstructural changes after aging at 500°C, 700°C, and 900°C for 100 min were observed using a JSM-6010LA SEM for certain alloy compositions.

Tensile properties were tested using an MTS810 materials testing machine, and fracture morphologies of tensile specimens were examined using a JSM-6010LA SEM. Alloy samples were machined by wire cutting into tensile specimens with a gauge length of 10 mm, thickness of 1.5 mm, width of 2.5 mm, and total length of 34 mm. To eliminate adverse effects of surface defects on mechanical properties, specimens were ground and polished to a bright finish. To eliminate machine error during tensile testing, BX120-2AA strain gauges were attached to the samples and connected to a JC-4a intelligent static strain indicator. The curves obtained from the strain indicator were fitted with those from the testing machine to obtain accurate stress-strain curves.

2.1 Effect of Thermite Composition on Microstructure

[Figure 2: see original paper] shows SEM images of the microstructures of samples synthesized from seven groups of thermites with different Al contents. [Figure 2: see original paper]a and b show SEM images of alloys synthesized with Al contents of 24.2% and 25.4% in the thermite, respectively. Both alloys consisted of dendrites with grain sizes of about 5-10 μm. XRD patterns ([Figure 3: see original paper]) indicated that the alloys were composed of fcc-structured austenite. EDS analysis results () showed that the alloys mainly contained Fe, Ni, Cr, and Al at this stage.

[Figure 2: see original paper]c shows the SEM image of an alloy synthesized with 26.6% Al in the thermite. The alloy consisted of equiaxed grains with diameters of 40-50 μm. EDS analysis () indicated that the alloy still mainly contained Fe, Ni, Cr, and Al. XRD patterns ([Figure 3: see original paper]) showed that when the Al content in the thermite exceeded 26.6%, the main constituent phase of the alloy changed from fcc-structured austenite to bcc-structured ferrite. At this point, three major diffraction peaks appeared at $2\theta = 44.50^\circ$, 64.75° , and 81.96° ,

which were overlapping peaks of bcc-structured ferrite and B2-structured NiAl intermetallic compound. The ferritic alloy and NiAl intermetallic compound have essentially the same crystal structure and very similar lattice constants, so their main peak positions basically coincide.

When the Al content in the thermite continued to increase to 27.8%, a large number of very fine granular precipitates began to appear inside the alloy grains, and fine lath-like structures formed at some grain boundaries ([Figure 2: see original paper]d). From the high-magnification SEM image of the intragranular structure ([Figure 2: see original paper]e), the granular precipitates appeared as square-shaped particles with sizes of 50-100 nm. Combined with XRD results, a weak superstructure diffraction peak appeared at $2\theta = 31.06^\circ$, indicating the presence of ordered NiAl phase, suggesting that the square-shaped dark particles were NiAl intermetallic compound. [Figure 2: see original paper]f and g show the microstructures of alloys synthesized with Al contents of 29.0% and 30.2% in the thermite, respectively. As the Al content in the thermite further increased, the lath-like structures originally present only at grain boundaries began to extend into the grains, forming large-area intertexture structures between grains, with some small grains entirely composed of intertexture structure. When the Al content in the thermite reached 31.4% ([Figure 2: see original paper]h and i), the alloy consisted of equiaxed grains pervaded by intertexture structure, with grain sizes of 20-30 nm.

[Figure 4: see original paper]a shows a TEM image of square-shaped precipitates inside a grain. The precipitates measured 50-100 nm in size. Selected-area electron diffraction (SAED) pattern analysis (inset in [Figure 4: see original paper]a) confirmed that the square-shaped precipitates were NiAl phase. [Figure 4: see original paper]b shows a TEM image of the intertexture structure, which consisted of alternating lath-like phases connected to each other. The dark region (matrix) had a width of 80-100 nm, while the light region had a width of about 50 nm. Combined with XRD analysis results ([Figure 3: see original paper]), the matrix was identified as bcc-structured ferrite phase, and the narrower lath phase was NiAl phase. The SAED pattern (inset in [Figure 4: see original paper]b) confirmed that the intertexture structure region consisted of bcc-structured ferrite phase and NiAl intermetallic compound, with an orientation relationship of $[001]_{\text{NiAl}} // [001]_{\text{ferrite}}$ and $(110)_{\text{NiAl}} // (110)_{\text{ferrite}}$ between NiAl phase and ferrite phase ($\alpha\text{-Fe}(\text{Ni}, \text{Cr})$), maintaining a coherent or semi-coherent relationship. [Figure 4: see original paper]c shows a TEM image of the transition region between the square-shaped precipitate region and the intertexture structure, revealing no distinct interface between the two microstructural regions.

2.2 Microstructural Evolution Mechanism

The reaction in this experiment involved many elements, making analysis of the FeNiCrAl quaternary alloy system complex. However, the existing FeNiAl ternary alloy system is similar to the FeNiCrAl system and can be used as a starting point for analysis. The binding force between Cr and Fe is much greater

than that between Cr and NiAl phases [7], so Cr preferentially combines with Fe to form γ -Fe(Ni,Cr) ferrite phase.

According to the 750°C horizontal and vertical section diagrams of the FeNiAl ternary phase diagram proposed by Bradley [16–18], δ represents the disordered bcc phase, β represents the ordered NiAl superstructure phase, and γ represents the austenite phase. In the thermite compositions used in this work, the atomic ratio of Fe to Ni was maintained at approximately 5:2. As the Al content increased, the composition point of the alloy in the phase diagram changed accordingly. When the Al content in the thermite did not exceed 25.4%, the composition point was located in the δ phase region of the phase diagram, and the main constituent phase of the alloy was austenite. In the thermite reaction, Al was insufficient while oxides were excessive. The low Al content prevented complete reduction of metal elements from various oxides, and most Al was removed from the alloy as Al₂O₃ slag.

As the Al content in the thermite continued to increase, the alloy composition point entered the coexistence region of δ and β phases in the phase diagram, corresponding to the observed region of γ -Fe(Ni,Cr) matrix coexisting with NiAl phase in this experiment. At this stage, Fe, Ni, and Cr existed in bcc form, while the B2-structured NiAl phase was coherent with bcc-structured γ -Fe(Ni,Cr). The low interfacial energy allowed extensive precipitation, achieving coherent precipitation strengthening.

When the Al content continued to increase, the shape of the β phase observed in this experiment changed from granular to intertexture. This intertexture structure first began to form at grain boundaries. The intertexture structure is very similar to typical spinodal decomposition microstructures (such as the spinodal structure of Fe–Ni–Mn–Al [19]) but differs significantly from microstructures formed through nucleation and growth processes. The region composed of δ + β phases represents a miscibility gap, indicating the immiscible region of the two phases, and the existence of a miscibility gap in the system is a prerequisite for spinodal decomposition. Therefore, it can be inferred that the formation mechanism of this intertexture structure is spinodal decomposition.

According to the theory proposed by Cahn [20–22], when inflection points appear in the composition-free energy curve of a system, uphill diffusion occurs within the inflection region, forming solute-enriched and solute-depleted zones that interconnect to create a network structure. During spinodal decomposition, although the new phase and parent phase maintain a coherent relationship, elastic strain arises between them due to differences in atomic radii of solute and solvent atoms. Since the elasticity of the alloy itself is anisotropic, the second-phase particles after spinodal decomposition tend to grow preferentially and rapidly along crystallographic directions with lower elastic strain resistance to reduce the system's free energy, resulting in a periodic network structure with perpendicular alignment between phases—that is, the intertexture structure.

Based on previous research results [23], it is believed that the spinodal decompo-

sition in this experiment occurred in the liquid phase, meaning that enrichment of Fe and Cr atoms and Ni and Al atoms already existed in the metallic melt while in the liquid state. Liquid-phase spinodal decomposition was first observed in oxide glasses [24], and recent experimental evidence indicates that liquid-phase separation in alloys occurs in deeply undercooled melts [25-27]. Under deep undercooling conditions, melt viscosity increases while the diffusion coefficient decreases, making liquid-phase separation possible in metals. In this experiment, the separation of Al₂O₃ slag from the melt purified the melt and created conditions for deep undercooling, while the extremely fast cooling rate of the melt also made liquid-phase spinodal decomposition possible. When the Al content in the thermite was between 27.8% and 30.2%, the solidification point at grain boundaries was lower, and the extremely fast cooling rate of the melt resulted in higher undercooling at grain boundaries, causing the intertexture structure to appear first at grain boundaries. As the Al content further increased, better thermodynamic and kinetic conditions for liquid-phase spinodal decomposition were satisfied, allowing the intertexture structure to pervade entire grains.

When TiO₂ gel was added to the thermite used in this work, numerous dispersedly distributed nanoscale Al₂O₃ particles were found in the synthesized alloy, and these nanoparticles were all symbiotic with NiAl intermetallic compound [23]. Since nanoscale Al₂O₃ particles can only move in the liquid melt, if spinodal decomposition occurred in the solid phase, the nanoscale Al₂O₃ particles should be uniformly distributed throughout the microstructure. Therefore, it is believed that before alloy solidification, two types of element-enriched zones—Fe, Cr and Ni, Al—had already formed, and the pre-precipitated Al₂O₃ particles moved to the Ni, Al element-enriched zones with lower interfacial energy due to interfacial energy and Brownian motion. This phenomenon provides strong evidence that spinodal decomposition in this experiment occurred in the liquid phase.

This work also preliminarily investigated the dimensional stability of NiAl phase during high-temperature aging. [Figure 5: see original paper] compares the microstructure before aging with those after aging at 500°C, 700°C, and 900°C for 100 min, showing that the alloy still maintained a relatively clear intertexture structure after aging. The NiAl phase size was between 60–80 nm, representing some growth compared to the as-synthesized alloy (50–60 nm). Taillard et al. [28] found that when the NiAl phase size is less than 300 nm, it can maintain a coherent or semi-coherent relationship with the matrix. Based on this analysis, under the experimental conditions of this work, the NiAl phase can still maintain a good coherent relationship with the ferrite matrix. More detailed studies on microstructural stability are ongoing.

2.3 Mechanical Properties

[Figure 6: see original paper] shows the tensile stress-strain curves of alloys with varying Al content in the thermite. The tensile strength of the alloys

first increased and then decreased with increasing Al content in the thermite, reaching a maximum of 640.87 MPa at 26.6% Al.

[Figure 7: see original paper] shows the variation trend of tensile strength and elongation after fracture with Al content in the thermite. The elongation after fracture consistently decreased as Al content increased, reaching 25.5% at 24.2% Al but only 1.7% at 29.0% Al.

Fracture morphologies of the alloys are shown in [Figure 8: see original paper]. At 24.2% Al in the thermite, the fracture surface consisted of numerous small dimples, indicating ductile fracture ([Figure 8: see original paper]a and b). At 26.6% Al, the fracture surface comprised many dimples and river-pattern features characteristic of cleavage ([Figure 8: see original paper]c and d). Combined with an elongation after fracture greater than 5%, the fracture mechanism was still ductile. At 29.0% Al, the fracture surface showed a stepped microstructure ([Figure 8: see original paper]e and f), indicating obvious brittle fracture.

At low Al content in the thermite, the synthesized alloy consisted of fcc austenite (γ -Fe(Ni,Cr)) without NiAl precipitates, exhibiting good ductility and toughness similar to austenitic stainless steel. When the alloy consisted of ferrite, numerous fine NiAl particle reinforcements precipitated, significantly improving alloy strength through precipitation strengthening, though with slight reductions in ductility and toughness. When the volume fraction of NiAl reinforcement further increased and formed an intertexture structure, alloy brittleness increased markedly. This is because NiAl intermetallic compound is a brittle phase at room temperature. When the volume fraction of brittle NiAl phase increased to nearly 50% and interconnected into parallel laths, cracks could easily propagate rapidly along the brittle NiAl phase once initiated, increasing alloy brittleness. Additionally, at higher Al content in the thermite, the synthesized alloy had larger grain sizes of 20–30 μm , which was another reason for the increased brittleness.

Literature reports [29] that the room-temperature tensile strength of heat-resistant austenitic stainless steel AISI 304 (containing 18% Cr, 8% Ni) is 585 MPa, that of heat-resistant ferritic stainless steel AISI 430 (containing 16–18% Cr) is 539 MPa, and that of corrosion-resistant superalloy Alloy 800 (containing 21% Cr, 32.5% Ni) is 600 MPa. Teng et al. [30] studied the room-temperature ductility of NiAl-phase-strengthened FeNiCrAl alloys (containing 10% Cr, 10% Ni) and found through three-point bending tests that when the Al mass fraction in the prepared alloy reached above 5%, the room-temperature elongation was less than 2%. The Fe(Ni,Cr)/NiAl alloy prepared by thermite synthesis in this work, when containing 26.6% Al in the thermite, exhibited a room-temperature tensile strength of 640.87 MPa and elongation of 11.1%, showing improved strength compared to traditional heat-resistant steels and significantly higher elongation than FeNiCrAl alloys strengthened by NiAl precipitation through aging.

Conclusions

- (1) At low Al content in the thermite, the main constituent phase of the alloy was austenite. As Al content increased, the main constituent phase changed from austenite to ferrite, accompanied by precipitation of granular NiAl phase. With further increase in Al content, the granular NiAl phase was gradually replaced by an intertexture structure.
- (2) The intertexture structure consists of γ -Fe(Ni,Cr) matrix and lath-shaped NiAl precipitates. The mechanism for formation of the intertexture structure is spinodal decomposition in the liquid phase during cooling.
- (3) As Al content in the thermite increased, the elongation after fracture of the alloy decreased, reaching 25.5% at 24.2% Al but only 1.7% at 29.0% Al. Meanwhile, the tensile strength first increased and then decreased, achieving a maximum of 640.87 MPa at 26.6% Al in the thermite.

References

- [1] Masuyama F. *ISIJ Int*, 2001; 41(6): 612
- [2] Calderon H, Fine M E. *Mat Sci Eng*, 1984; 63(2): 197
- [3] Pearson W B. *Handbook of lattice spacing and structure of metals*. Oxford: Pergamon Press, 1958:347
- [4] Stallybrass C, Schneider A, Sauthoff G. *Intermetallics*, 2005; 13(12): 1263
- [5] Sudbrack C K, Yoon K E, Noebe R D, Seidman D N. *Acta Mater*, 2006; 54(12): 3199
- [6] Calderon H A, Fine M E, Weertman J R. *Metall Trans A*, 1988; 19(5): 1135
- [7] Hao S M, Ishida K, Nishizawa T. *Metall Trans A*, 1985; 16A:179
- [8] Stallybrass C, Sauthoff G. *Mat Sci Eng A*, 2004; 387: 985
- [9] Vo N Q, Liebscher C H, Rawlings M J, Asta M, Dunand D C. *Acta Mater*, 2014; 71: 89
- [10] Bradley A J, Taylor A. *Proc Roy Soc*, 1938; 166(926): 353
- [11] Yin S. *Combustion Synthesis*. Beijing: Metallurgical Industry Press, 2004:1 (殷声. 燃烧合成. 北京: 冶金工业出版社, 2004: 1)
- [12] Borovinskaya I P. *Pure Appl Chem*, 1992; 64(7): 919
- [13] Yukhvid V I. *Pure Appl Chem*, 1992; 64(7): 977
- [14] Fu Z. *Acta Mater Comp Sin*, 2000; 17(1): 5 (傅正义. 复合材料学报, 2000; 17(1): 5)
- [15] Hao S M, Takayama T, Ishida K, Nishizawa T. *Metall Trans A*, 1984; 15(10): 1819
- [16] Bradley A J. *J Iron Steel Inst*, 1949; 163(1): 19
- [17] Bradley A J. *J Iron Steel Inst*, 1951; 168: 233
- [18] Bradley A J. *J Iron Steel Inst*, 1952; 171(1): 41
- [19] Hanna J A, Baker I, Wittmann M W, Munroe P R. *J Mater Res*, 2005; 20(04): 791
- [20] Cahn J W. *Acta Metall*, 1961; 9(9): 795
- [21] Cahn J W. *Acta Metall*, 1962; 10(3): 179

- [22] Cahn J W. Acta Metall, 1962, 10(10): 907
- [23] Xi W, Peng R L, Wu W, Li N, Wang S, Johansson S. J Mater Sci, 2012; 47(8): 3585
- [24] Zhang C, Yao K. Acta Metall Sin, 2006; 42(8): 870 (张长青, 姚可夫. 金属学报, 2006; 42(8): 870)
- [25] Ma N, Kui H W. China Mech Eng, 2000; 11(11): 1298 (马南钢, Kui H W. 中国机械工程, 2000; 11(11): 1298)
- [26] Lee K L, Kui H W. J Mater Res, 1999; 14(09): 3653
- [27] Yuen C W, Lee K L, Kui H W. J Mater Res, 1997; 12(02): 314
- [28] Taillard R, Pineau A, Thomas B J. Mater Sci Eng, 1982; 54(2): 209
- [29] Rothman M F. High-temperature property data: ferrous alloys. ASM International, 1987:250
- [30] Teng Z K, Liu C T, Ghosh G, Liaw P K, Fine M E. Intermetallics, 2010; 18(8): 1437

Note: Figure translations are in progress. See original paper for figures.

Source: ChinaXiv – Machine translation. Verify with original.